Supplementary information for

Protein-based Sensitive, Selective and Rapid Fluorescence Detection of Picric Acid in Aqueous Media

Xiangcheng Sun,[a] Xiaoyu Ma,[b] Challa Vijaya Kumar,[c] and Yu Lei[a*]

[a]Department of Chemical and Biomolecular Engineering
[b]Department of Biomedical Engineering
[c]Department of Chemistry, Department of Molecular and Cell Biology, Institute of Materials Science
University of Connecticut, Storrs, Connecticut, 06269, USA.
Email: ylei@engr.uconn.edu

Experimental section

Reagents. Bovine serum albumin (BSA, ≥98%, agarose gel electrophoresis lyophilized) was purchased from Sigma Aldrich. Sodium phosphate buffer (0.01 M, pH=7.4) was used for preparation of BSA solution. Nitro based explosives such as picric acid (PA, ≥99%), 2,4-dinitrotoluene (DNT, 97%), 1,3-dinitrobenzene (DNB, ≥99%), 2,4-dinitrophenol (DNP, ≥98%), 4-nitrophenol (4-NP, 99%), and 3-nitrophenol (3-NP, 99%) were purchased from Sigma Aldrich. 1,3,5-trinitroperhydro-1,3,5-triazine (RDX) (1000 µg/mL in acetonitrile) was bought from Chem Service. 2,4,6-trinitrotoluene (TNT, 1000 µg/mL in acetonitrile), 2,4,6-trinitrophenylmethylnitramine (Tetryl, 1000 µg/mL in acetonitrile) was obtained from Ultra Scientific, while nitromethane (NM, 99+%) was bought from Acros Organics. 2-Nitrotoluene (2-NT, ≥99.0%) was obtained from Fluka. Octogen (HMX, 1000 µg/mL in acetonitrile: methanol) was purchased from SPEX CertiPrep. Pentaerythritol tetranitrate (PETN, 1000 µg/mL in acetonitrile) was bought from Cerilliant.

Equipment. The absorption spectra were performed on a Cary 50 UV-vis spectrophotometer (Agilent Technologies). Fluorescence emission spectra were measured using a Varian Cary Eclipse fluorescence spectrometer (Agilent Technologies). Circular dichroism measurements were conducted on a JASCO (J-710) spectropolarimeter by fixing the concentrations of BSA while varying the analyte concentrations.

Detection of nitro explosives in aqueous samples. The sensing experiments were carried out by monitoring the fluorescence quenching behavior of BSA solution upon the addition of target explosives at room temperature through a fluorescence spectrometer, in which the excitation and emission slits width were adjusted according to the fluorescence intensities. Briefly, 3 mL of BSA solution was placed in a disposal cuvette and then the target solution was added successively. Each titration was repeated at least three times and consistent results are reported. The fluorescence emission experiments were excited at 279 nm, and the emission data were collected in the wavelength range of 290-450 nm. The quenching percentage (QP) was calculated using the equation as follows:

$$QP\ \% = (1 - I/I_0) \times 100\%$$

where I_0 is the initial fluorescence intensity in the absence of analyte, I is the fluorescence intensity in the presence of corresponding analyte.

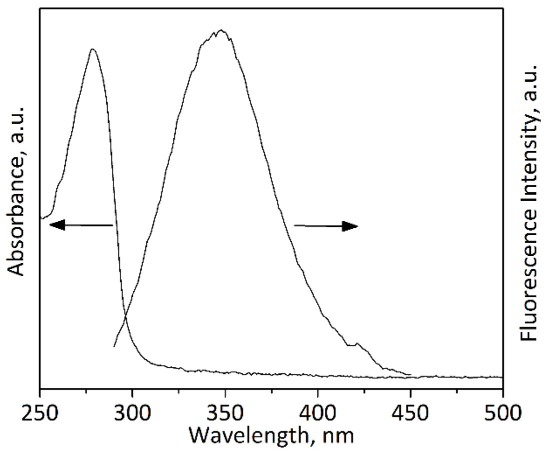

Fig. S1 Absorption and emission spectra of BSA solution (emission spectrum upon excitation at 279 nm).

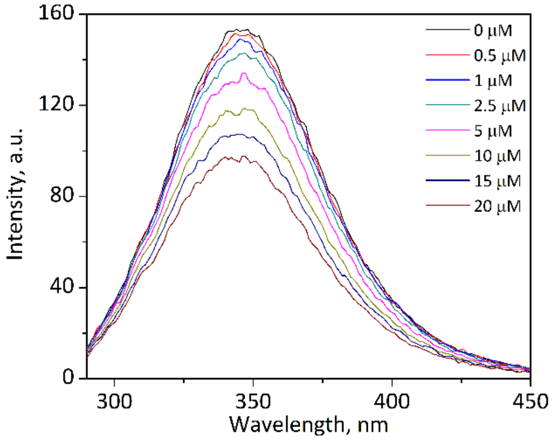

Fig. S2 Fluorescence spectra of BSA upon addition of Tetryl in aqueous solution.

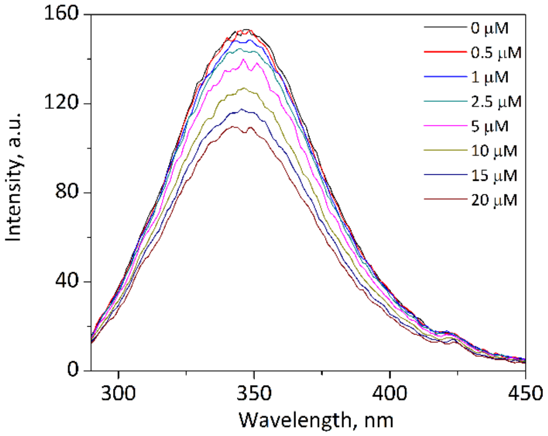

Fig. S3 Fluorescence spectra of BSA upon addition of 2-NT in aqueous solution.

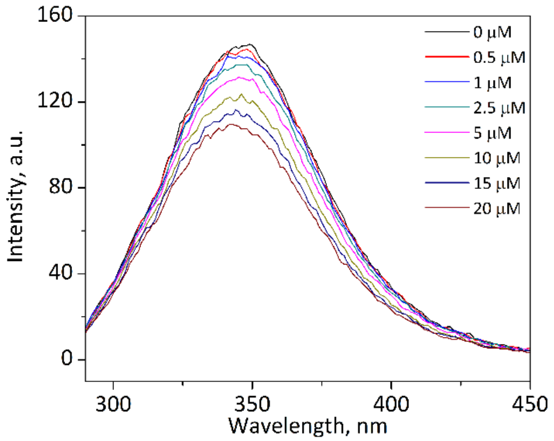

Fig. S4 Fluorescence spectra of BSA upon addition of TNT in aqueous solution.

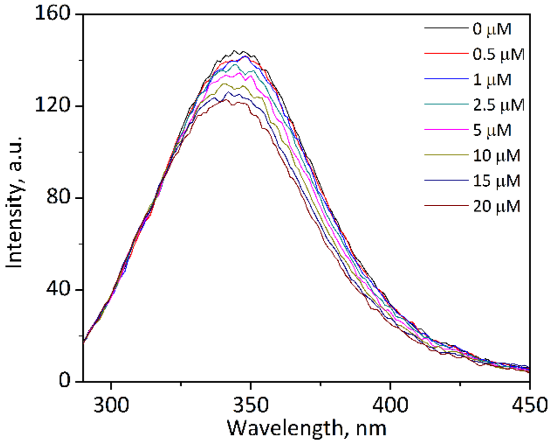

Fig. S5 Fluorescence spectra of BSA upon addition HMX of in aqueous solution.

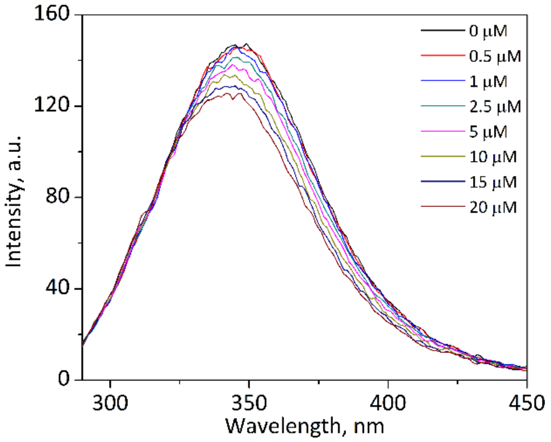

Fig. S6 Fluorescence spectra of BSA upon addition of PETN in aqueous solution.

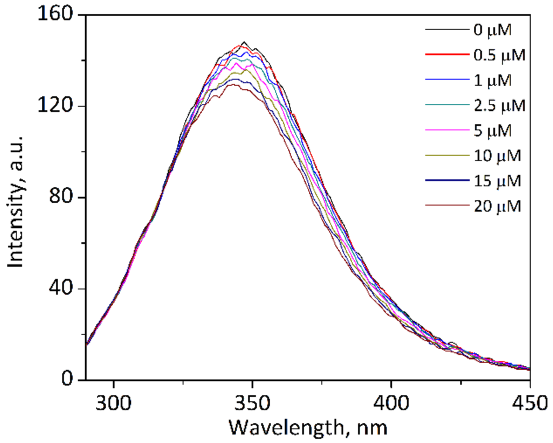

Fig. S7 Fluorescence spectra of BSA upon addition RDX of in aqueous solution.

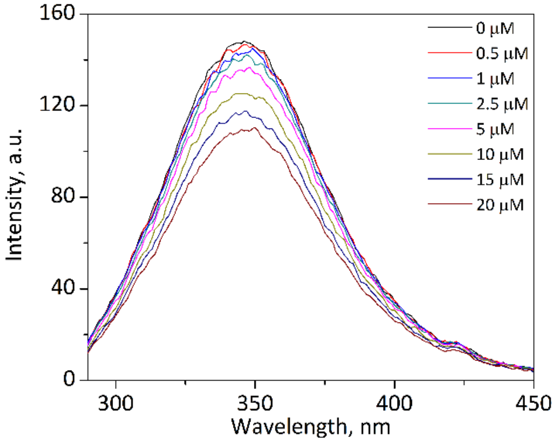

Fig. S8 Fluorescence spectra of BSA upon addition of DNT in aqueous solution.

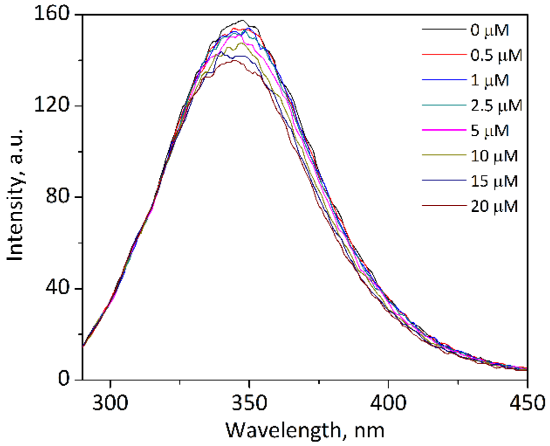

Fig. S9 Fluorescence spectra of BSA upon addition of DNB in aqueous solution.

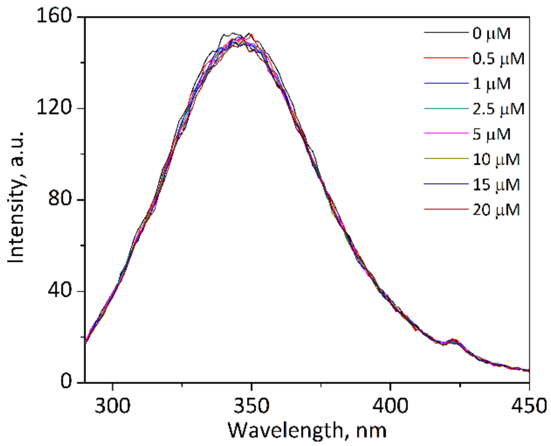

Fig. S10 Fluorescence spectra of BSA upon addition of NM in aqueous solution.

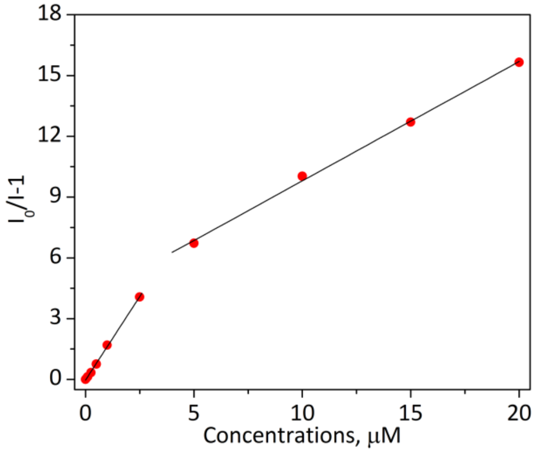

Fig. S11 Linear fitting of Stern-Volmer plot for PA explosive detection using 0.5 μM BSA.

The Stern-Volmer plot for PA in 0.5 μM BSA solution was shown in Fig. S11, and the fitting parameters were obtained. The S-V plot is nearly linear at low concentrations and deviates downward from linearity in a higher concentration range. In the low concentration range, the K_{SV} value was calculated as 1.65×10^6 M^{-1}, and the correlation coefficient R^2=0.999; In the high concentration range, the K_{SV} value was calculated as 5.90×10^5 M^{-1}, and the correlation coefficient R^2=0.997.

The efficiency of energy transfer between the donor and the acceptor, E, could be calculated by the following equation[1-3]:

$$E = 1 - \frac{F}{F_0} = \frac{R_0^6}{R_0^6 + r_0^6} \qquad (1)$$

where r_0 represents the distance between the donor and acceptor, and R_0 is the critical distance at which energy transfer efficiency equals to 50%. The value of R_0 is calculated using the equation:

$$R_0^6 = 8.79 \times 10^{-5} K^2 n^{-4} \emptyset J(\lambda) \text{ (in Å}^6\text{)} \tag{2}$$

Where K^2 is the orientation factor related to the geometry of the donor-acceptor dipole, n is the refractive index of the medium, $\emptyset$ is the fluorescence quantum yield of the donor, and J(λ) in M^{-1} cm^{-1} nm^4, expresses the degree of spectral overlap between the donor emission and the acceptor absorption, J(λ) is given by:

$$J(\lambda) = \frac{\int_0^\infty F(\lambda)\varepsilon(\lambda)\lambda^4 d\lambda}{\int_0^\infty F(\lambda) d\lambda} \tag{3}$$

Where F(λ) is the corrected fluorescence intensity of the donor in the wavelength λ to λ+Δλ, ε(λ) is the extinction coefficient of the acceptor at λ in M cm^{-1}. In the present case, K^2 =2/3, n=1.36, and $\emptyset$=0.15. When C(PA)=C(BSA)=0.50 μM, E=0.432, according to Eqs. (1)-(3), we could calculate that J(λ) for picric acid, J(λ)=1.16×10^{14} M^{-1} cm^{-1} nm^4, R_0=2.58 nm, and r_0=2.70 nm. The degree of spectra overlap J(λ) for other analytes were also calculated and the results were shown in Table S4.

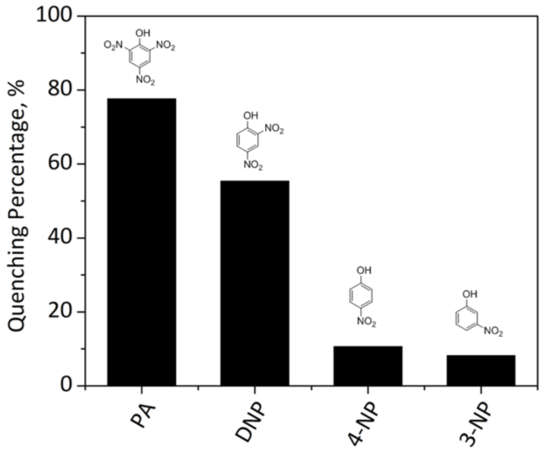

Fig. S12 Comparison of quenching percentage of BSA fluorescent sensors upon addition of various 2.5 μM nitrophenols.

As shown in Fig. S12, the quenching efficiency follows the order PA>DNP>4-NP>3-NP, which is in complete agreement with the order of acidity of these analytes, where the pKa values of the quenchers are 0.38 for PA, 4.89 for DNP, 7.15 for 4-NP, and 8.4 for 3-NP. In addition, the quenching efficiency of PA and DNP are much higher than their corresponding structure-similar nitro compounds (TNT, DNT and DNB). This feature when coupled with the magnitudes of the overall integrals may explain the molecular basis for the unprecedented selectivity for PA, as other nitro compounds do not have a hydroxyl group and so they cannot interact efficiently with amino groups of BSA and so result in a very low quenching efficiency. In addition, the interaction of the hydroxyl groups with the basic sites in BSA is expected to follow the order of their acidity.

Table S1 Comparison of present results with previous fluorescent picric acid sensors

Reference	K_{SV} (M^{-1})	Detection limit	Selectivity
J. Mater. Chem., 2009, 19, 7347	/	4.8 ppb	High
Adv. Funct. Mater., 2009, 19, 905;	1.09×10^5	0.2 ppm	High
Macromol. Rapid. Commun. 2010, 31, 834	9.09×10^3	1 ppm	/
Chem. Commun., 2011, 47, 4505	/	98.5 ppb	High
Chem. Commun., 2011, 47, 10046	2100	/	Low
J. Photochem. Photobiol., A 2011, 217, 356	5×10^4	2.3 ppb	Low
ACS Appl. Mater. Interfaces 2011, 3, 1245	5.7×10^3	70 ppb	High
Inorg. Chem. 2011, 50, 1506	1×10^5	/	Low
Inorg. Chem. 2012, 51, 13072	/	/	Low
Chem. Commun., 2012, 48, 7167	2.5×10^5	0.4 ppm	Low
J. Mater. Chem., 2012, 22, 11574	3.04×10^4	23 ppb	Moderate
Anal. Chem., 2012, 84, 8415	/	32.3 ppb	High
Chem. Commun., 2012, 48, 5007	9.9×10^4	3-300 ppb	Low
Angew. Chem. Int. Ed., 2013, 52, 2881	3.5×10^4	0.916 ppm	High
ACS Appl. Mater. Interfaces, 2013, 5, 672	1.55×10^4	80.2 ppb	Moderate
ACS Appl. Mater. Interfaces, 2013, 5, 5373.	3.2×10^6	0.9 ppb	High
Chem. Commun., 2013, 49, 4764.	1.9×10^4	/	High
J. Am. Chem. Soc., 2013, 135, 17310;	7.8×10^4	1 ppm	High
J. Org. Chem., 2013, 78, 1306	3.8×10^4	/	High
Chem. Commun., 2014, 50, 6031	5.28×10^4	/	Moderate
ACS Applied Mater. Inter. 2014, 6, 10722	1.32×10^5	125 ppb	High
Asian J. Org. Chem. 2014, 3, 805	3.57×10^5	0.23 ppb	High
Present Study	$\mathbf{1.65\times10^6}$	**3.9 ppb**	**Very high**

Table S2 Fluorescent quenching constant K_{SV} values for the various explosive analytes

Analytes	K_{SV} (M^{-1})
PA	1.65×10^{6}
Tetryl	2.85×10^{4}
TNT	1.64×10^{4}
DNT	1.77×10^{4}
2-NT	1.98×10^{4}
DNB	5.39×10^{3}
NM	/
RDX	5.62×10^{3}
PETN	7.92×10^{3}
HMX	7.86×10^{3}

Table S3 LUMO and HOMO energies calculated for the various explosive analytes (at the B3LYP/6-31G* level of theory)[4-6]

Analytes	LUMO (eV)	HOMO (eV)	Band gap (eV)
PA	-3.89(-4.32)	-8.22(-8.60)	4.33(4.28)
Tetryl	-3.92	-8.11	4.19
TNT	-3.48	-8.44	4.96
DNT	-2.97	-8.11	5.14
2-NT	-2.75	-7.56	4.81
DNB	-3.43	-7.99	4.56
NM	-1.90	-8.03	6.13
RDX	-2.53	-8.25	5.71
PETN	-3.08	-8.71	5.63
HMX	-2.72	-8.30	5.58

Table S4 Degree of spectra overlap integral J(λ) values for the various explosive analytes.

Analytes	J(λ) (M^{-1} cm^{-1} nm^{4})
PA	1.16×10^{14}
Tetryl	8.42×10^{12}
TNT	7.10×10^{12}
DNT	6.10×10^{12}
2-NT	1.19×10^{13}
DNB	2.12×10^{12}
NM	7.84×10^{11}
RDX	7.72×10^{11}
PETN	9.82×10^{12}
HMX	1.08×10^{12}

References

1. J. R. Lakowicz, *Principles of Fluorescence Spectroscopy*, Springer, Singapore, 2006.
2. N. Shahabadi and M. Maghsudi, *J. Mol. Struct.*, 2009, **929**, 193-199.
3. Y.-Z. Zhang, X. Xiang, P. Mei, J. Dai, L.-L. Zhang and Y. Liu, *Spectrochim. Acta, Part A*, 2009, **72**, 907-914.
4. J. C. Sanchez, A. G. DiPasquale, A. L. Rheingold and W. C. Trogler, *Chem. Mater.*, 2007, **19**, 6459-6470.
5. S. S. Nagarkar, B. Joarder, A. K. Chaudhari, S. Mukherjee and S. K. Ghosh, *Angew. Chem. Int. Ed.*, 2013, **52**, 2881-2885.
6. Z. Hu, B. J. Deibert and J. Li, *Chem. Soc. Rev.*, 2014, http://dx.doi.org/10.1039/C1034CS00010B.